C.R. Acad. Sci. Paris,
t. 322, série II *a*,
p. 407 à 413,
1996

Stability of a density-stratified two-layer system

Patrick Massin, Nicolas Triantafyllidis and Yves M. Leroy

N. T. : Department of Aerospace Engineering University of Michigan, Ann Arbor, MI, USA ;
Y. M. L. and P. M. : Laboratoire de Mécanique des Soli École Polytechnique, URA CNRS No. 317, 91128 Palaiseau, France.

Abstract The results of a linear and a non-linear stability analysis are presented for the system composed of a cohesive, frictional overburden resting on a viscous substratum of lower density. Stability depends on the *in situ* stress and not solely on the density contrast, as for visco-elastic models. It is shown that an unstable system evolves towards a stable fold whose finite amplitude is a function of the tectonic force. However, if faulting occurs in the overburden during the fold development, the structure then collapses in a chevron mode.

Keywords: Instability, Fold, Chevron, Fault, Large strain.

Résumé **Stabilité d'un système à deux couches stratifié en densité**

Les résultats présentés concernent la stabilité linéaire et non-linéaire du système stratifié, composé d'un matériau à cohésion et à friction reposant sur un fluide visqueux de moindre densité. La stabilité dépend de la contrainte tectonique et pas seulement du contraste de densité comme pour les modèles visco-élastiques. Le système initialement instable évolue vers un nouvel équilibre : un pli dont l'amplitude finie est fonction de la contrainte tectonique. Cependant, si l'initiation de failles dans le solide se produit lors de ce développement, une ruine du système stratifié en un mode de chevron est observée.

Mots-clés : Instabilité, Pli, Chevron, Faille, Grande déformation.

Version française abrégée

Le modèle bidimensionnel considéré consiste en deux couches horizontales (fig. 1). Les propriétés du matériau de la couche supérieure sont décrites par le modèle élasto-plastique de Rudnicki et Rice (1975) qui prend en compte les grandes déformations. La couche inférieure contient un fluide de viscosité constante et de densité inférieure à celle du solide. Les effets de pression de pore et de viscosité dans la couche supérieure sont négligés. Une condition de glissement sans frottement est imposée entre la couche inférieure et le socle rigide. Les contraintes, dans la couche supérieure, dans les directions 1 et 3 ont pour gradient k_1 et k_3 fois le gradient lithostatique, respectivement; la contrainte à l'interface entre les deux couches dans les directions 1 et 3 est notée $\sigma_0 \cos(\varphi)$ et $\sigma_0 \sin(\varphi)$. La contrainte dans le fluide résulte de la pression hydrostatique et lithostatique. L'hypothèse d'un chargement proportionnel et l'adoption d'une loi puissance pour la courbe contrainte-déformation permettent de calculer la déformation permanente associée à la contrainte *in situ*, en tout point de la couche supérieure.

Une analyse de stabilité linéaire de ce système de longueur infinie a été présentée par Leroy et Triantafyllidis (1995). Elle est fondée sur l'hypothèse qu'une perturbation ne peut induire de décharge élastique, si une déformation plastique est associée à la contrainte *in situ*. Les résultats de l'analyse linéaire sont présentés en figure 2 sous la forme d'isocontours de coefficient de stabilité, dans un espace décrit par le nombre d'onde sans dimension

Note

présentée par
Paul Tapponnier.

remise le 13 novembre 1995,
acceptée après révision le 8 janvier 1996.

ω H_a et la contrainte σ_0 normalisée par la cohésion. Notons l'existence d'états stables ainsi que d'une longueur d'onde à croissance maximum pour toute contrainte supérieure à σ_T. Ces résultats s'appliquent à un système de taille finie – pour lequel une analyse de stabilité par les éléments finis est réalisée – si la longueur d'onde de la perturbation est un sous-multiple de la longueur de la structure. L'épaisseur de la couche supérieure est choisie dans ce qui suit, de telle façon qu'une perturbation de longueur d'onde égale à la longueur de la structure ait pour nombre d'ondes sans dimension $(\omega H_a)^*$ (*voir* **fig. 2**). Pour cette géométrie, le système est stable si σ_0 est plus petit que σ_T. Pour une valeur de σ_0 suffisamment grande, des perturbations de grand nombre d'ondes (e.g. 2 $(\omega H_a)^*$) ont une croissance plus rapide que la perturbation associée à $(\omega H_a)^*$; ceci est illustré par les points 2 et 3 de la figure 2.

Les résultats numériques obtenus reposent sur une formulation Lagrangienne avec coordonnées convectives, afin de tenir compte des grandes transformations (Massin, 1995). Le nombre sans dimension T est introduit comme le rapport du temps caractéristique du chargement sur le temps de relaxation du fluide visqueux. Ce dernier, noté t_R, correspond à la viscosité du fluide, divisée par le module d'élasticité en cisaillement du solide. L'équilibre correspond à T égal à zéro; un chargement passif, réalisé en augmentant de façon monotone la force ou le déplacement de la paroi latérale (**fig. 1**), requiert que T soit petit devant l'unité.

L'évolution d'un état d'équilibre perturbé ne correspond pas aux prédictions de l'étude linéarisée, en raison d'une décharge élastique partielle dans la couche supérieure : la stabilité neutre n'est pas détectée pour une contrainte σ_T, mais pour une contrainte plus grande σ_R. La prise en compte d'une compression passive lors de l'analyse numérique permet de retrouver les résultats de l'analyse linéaire. Une comparaison entre ces deux analyses est présentée en figure 3 pour les conditions initiales correspondant au point 1 de la figure 2. Lorsque la contrainte *in situ* est comprise entre σ_T et σ_R, la vitesse de croissance des perturbations est positive, mais reste de l'ordre de la vitesse de compression imposée par les conditions aux limites. Ce n'est que pour une contrainte supérieure à σ_R, que la vitesse de croissance des perturbations n'est plus gouvernée par la compression passive.

Le développement de l'instabilité à partir d'un équilibre ne conduit pas à la ruine du système, mais à la formation d'un pli d'amplitude finie, **fig. 4**. La sélection de ce nouvel équilibre dépend de la contrainte tectonique, ainsi que du type de conditions aux limites, **fig. 5**. Notons que la couche supérieure est entièrement élastique lorsque le pli est formé. La restabilisation ne se produit pas si des failles sont initiées (perte d'ellipticité, Rice, 1976) dans la couche supérieure. Dans ce cas, des rotules plastiques se développent à la crête et au creux du pli qui prend la forme d'un chevron. Le chevron présenté en figure 6 a été obtenu grâce à deux perturbations similaires à celles des points 2 et 3 de la figure 2. La perturbation de courte longueur d'onde a eu la croissance la plus rapide. Le chevron n'est pas un état d'équilibre stable, si la force est maintenue constante à la frontière latérale. La prise en compte de la compression passive ne change pas le développement de l'instabilité décrit ci-dessus. La seule différence est que le pli, une fois formé, continue de se développer à une vitesse déterminée par les conditions aux limites.

1. INTRODUCTION AND DESCRIPTION OF MODEL PROBLEM

The two-dimensional model problem considered consists of two horizontal layers resting on a rigid basement (**fig. 1**). The overburden is composed of a cohesive, frictional solid whose properties are described by the finite-strain, pressure-sensitive elasto-plastic model of Rudnicki and Rice (1975). Effects of pore fluid are disregarded by setting the pore pressure to zero. The substratum material is a fluid with a constant visco-

sity and a density lower than that of the overburden solid. The rate-controlling mechanism during the evolution of this stratified system is assumed to depend on the fluid viscosity and, consequently, any strain-rate sensitivity of the overburden material is disregarded. A condition of slip with no friction is assumed between the substratum and the rigid basement. The *in situ* stress distributions in direction 1 and 3 in the overburden are characterized by a vertical gradient, respectively, k_1 or k_3 times the lithostatic pressure gradient; the stress along directions 1 and 3 at the interface between substratum and overburden are $\sigma_0 \cos(\varphi)$ and $\sigma_0 \sin(\varphi)$, respectively. The substratum sustains a hydrostatic stress resulting from the lithostatic and hydrostatic pressures.

The choice of an elasto-plastic model for the overburden renders possible the study of various modes of instabilities such as folding and faulting. The onset of faulting, signalled by the loss of ellipticity of the governing equations (Rice, 1976), cannot be predicted with classical viscous-fluid models, which lack one of the appropriate destabilizing mechanisms responsible for faulting (Poirier, 1980). This deficiency is alleviated with non-associated elasto-plasticity models that allow certain stress states to lead to a loss of ellipticity in the positive work-hardening range of deformation (Rudnicki and Rice, 1975).

The need to develop a solution to the folding problem for elasto-plastic models has several motivations. The prediction of the initiation of distributed fracture in a fold requires the application of a fracture criterion and the knowledge of the stress state (Price and Cosgrove, 1990). To this end, an elasto-plastic model is an attractive alternative to the viscous-fluid approach considered by Lemiszki *et al.* (1994). It predicts the anisotropic development of a population of faults or defects, whose initial size is small compared to the fold dimensions (Lehner and Kachanov, 1995), prior to the onset of faulting at the length scale of the fold. Another motivation stems from the study of laboratory analogue models, such as those composed of viscous and granular materials in sandboxes, which seek to reproduce faulting in the competent layer. A linear and non-linear stability analysis, such as the ones reported here, will establish the differences between the initial development of instabilities (prior to major faulting) in the analogue model and the corresponding field case, shedding new light on accepted scaling rules.

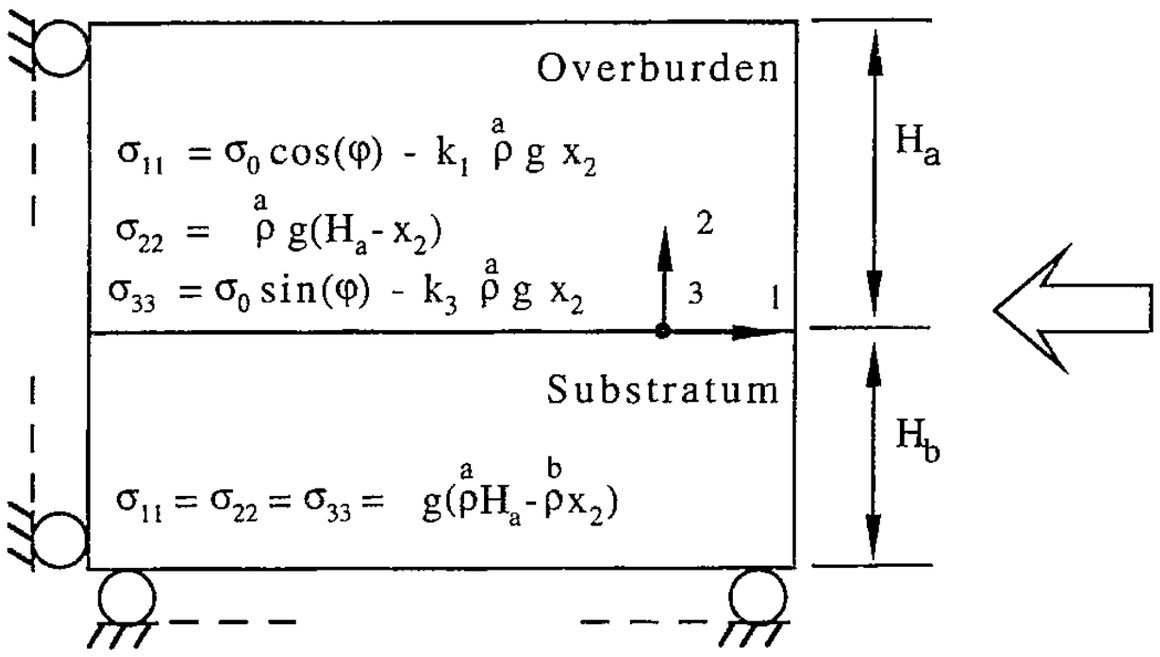

Fig. 1 Geometry of the model proble and *in situ* stress distribution. The density of the overburden and of the substratum are, respectively, denoted by $\overset{a}{\rho}$ and $\overset{b}{\rho}$.

Géométrie du problème et distribution de contrainte. L'épaisseur et la densité des couches supérieure et inférieure sont notées par H_a, $\overset{a}{\rho}$ et par H_b, $\overset{b}{\rho}$, respectivement.

The rest of this Note is organized as follows. Sections 2 and 3 pertain to the linear and non-linear stability analysis of the stratified system, respectively. The non-linear analysis reveals the importance of an elastic unloading at the onset of instability, which is ignored in the linear analysis, and establishes that the initially unstable stratified system evolves towards a new equilibrium in the form of a finite-amplitude fold. That amplitude is function of the magnitude of the compressive *in situ* stress. The emerging fold

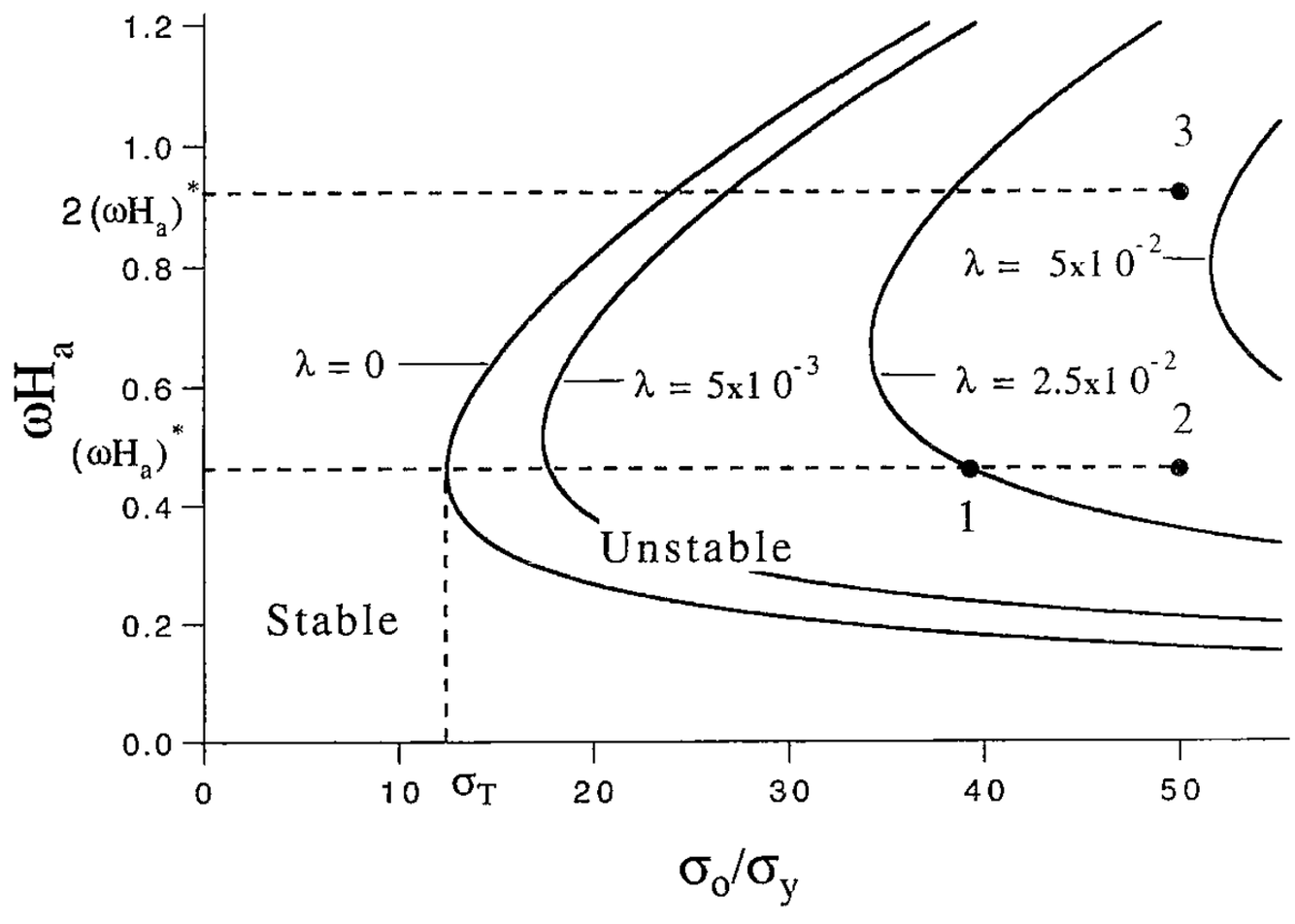

Fig. 2 Isocontours of dimensionless stability exponent λ in a space spann by the dimensionless wavenumber ωH_a and stress σ_0 normalized with respect to the cohesion σ_y.

Isocontours de coefficient de stabilité adimensionalisé dans l'espace décrit par les nombres d'ondes adimensionalisés ωH_a et la contrainte σ_0 normalisée par la cohésion σ_y.

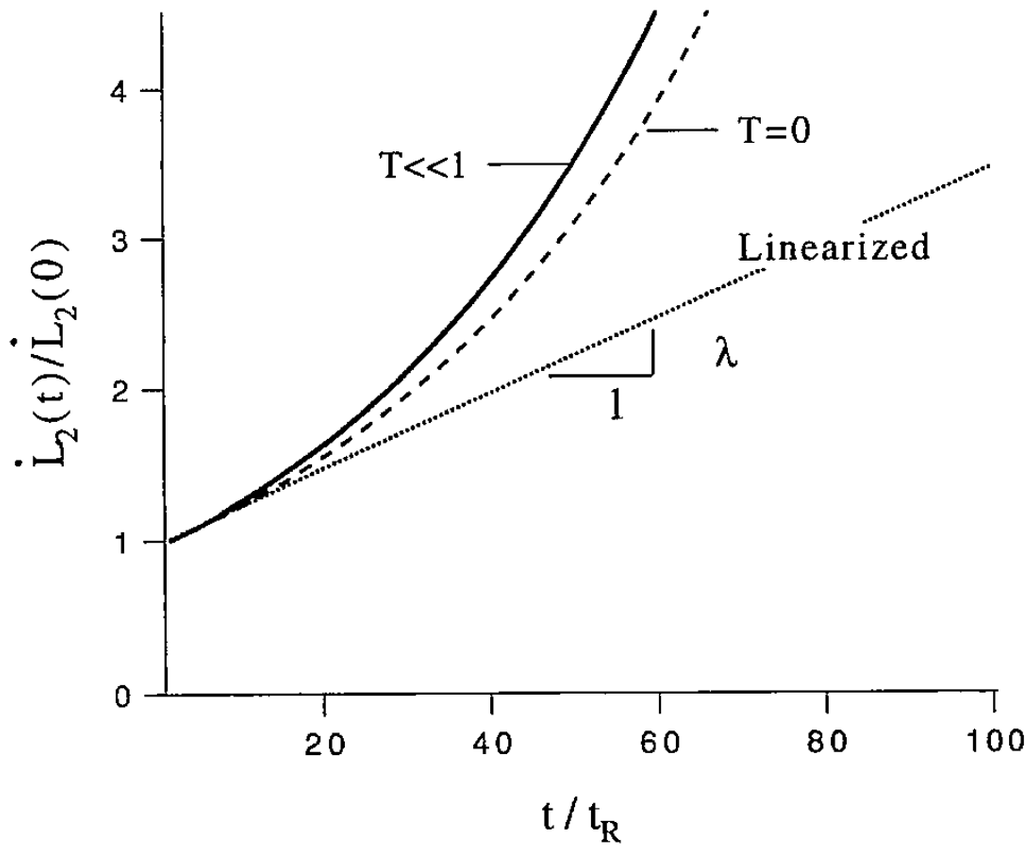

Fig. 3 Evolution with time of the perturbation amplitude growth rate for a stress σ_0 larger than σ_R. The solid, dotted and dashed curves, respectively, correspond to a passive compression, the associated predictions of the linear stability analysis and the evolution from an equilibrium state.

Evolution dans le temps de la vitesse de croissance d'une perturbation pour une contrainte σ_0 plus grande que σ_R. Les courbes continues, en pointillés longs et courts, correspondent aux résultats obtenus avec une compression passive, aux predictions de l'analyse linéaire et à l'évolution à partir d'un équilibre, respectivement.

transforms into a chevron if faulting occurs at its crest and trough. This Note is concluded by a discussion in section 4.

2. LINEAR STABILITY ANALYSIS

The linear stability analysis of the stratified system of infinite lateral extent makes use of the methodology developed by Biot (1965) for solids under initial stress and subsequently applied to bifurcation problems for elasto-plastic materials by, e.g., Hill and Hutchinson (1975). Neutral stability results for a stratified system with an infinitely deep substratum have been reported by Triantafyllidis and Leroy (1994). An asymptotic solution to the same problem–except that the substratum thickness is taken to be finite–has been presented and validated by the same authors for the whole unstable range of wavelength and tectonic force (Leroy and Triantafyllidis, 1995; Triantafyllidis and Leroy, 1995). In these analyses the state of stress described in figure 1 is assumed to be reached by proportional loading; the accumulated plastic deformation is computed according to this loading path with the same power law for the stress-strain curve at every point of the overburden. It is further assumed that a perturbation induces a plastic straining if the *in situ* stress has already generated a permanent deformation. A possible elastic unloading upon perturbation is thus disregarded.

Typical results of the linear analysis are presented in figure 2 for a substratum to overburden thickness ratio H_b/H_a of 9. The data used to obtain these results are found in the references cited above. The various curves are isocontours of dimensionless stability exponent λ, (*i.e.*, the rate of growth of the instability if positive) in a space spanned by the dimensionless wavenumber ωH_a and the normalized stress σ_0. Note the isocontour of neutral stability ($\lambda = 0$) and the existence of a range of wavenumbers that lead to instability for any given stress larger than a certain stress, denoted by σ_T for reasons given in the concluding section. In that range there is a perturbation with fastest growth. The striking difference between the results presented in figure 2 and any stability results based on the visco-elastic model (e.g., Biot and Odé, 1965) is the existence of stable states like those for an elastic beam on a viscous foundation. Our results are more realistic than those of the beam model, however, since we take into account a non-linear rheology, a realistic *in situ* stress distribution in the overburden and geometric effects due to the prestress.

The results of the linear stability analysis are applicable to the case of a stratified system of finite lateral extent–for which we conducted a finite-element stability analysis–if the length of the structure is a multiple of the perturbation wavelength. In what follows, the overburden thickness and the perturbation wavelength are chosen such that the value of ωH_a corresponds to the ordinate of the furthest left point on the neutral stability curve, $(\omega H_a)^*$, in figure 2. The abscissa of that point is σ_T. Hence, for that particular structure, stability is guaranteed if the *in situ* stress σ_0 is less than σ_T. Note that for large values of σ_0 compared to σ_T, perturbations with shorter wavelengths are also unstable. This is illustrated in figure 2 in which point 3 corresponds to a perturbation half the wavelength of the perturbation at point 2.

3. NON-LINEAR STABILITY ANALYSIS

The numerical results presented in this section are based on the finite-element method (Massin, 1995). A fully Lagrangian formulation of the governing equations is adopted, with the convected-coordinates approach discussed by Hutchinson (1973) to account for large strains. The finite elements are four-noded and isoparametric with the displacements as nodal unknowns. The mean-dilatation method is employed in view of the nearly incompressible response of the material in the overburden and in the substratum.

The dimensionless number T is defined as the ratio of the characteristic time associated with the loading rate to the one associated with the fluid relaxation. The latter, denoted by t_R, is defined as the viscosity of the fluid divided by the modulus of elasticity in shear of the overburden material. Loading is performed by increasing with time the total applied force or the displacement at the lateral boundary (**fig. 1**). An equilibrium corresponds to T equal to zero and a passive compression requires T to be small compared to one.

The initial evolution of a perturbed equilibrium ($T = 0$) with an *in situ* stress σ_0 greater than σ_T does not correspond to the predictions of the linear stability analysis. This discrepancy arises from the elastic unloading that is always induced when the stratified system is perturbed; the distribution of material points unloading elastically and loading plastically takes the form of a chessboard in the overburden. It is found that the stress σ_0 has to be larger than a critical stress, denoted by σ_R for reasons to be explained later, for the initial rate of growth to be positive. It is only in the presence of a passive compression ($T \ll 1$) that the rate of growth at the onset of instability is precisely the one predicted by the linear analysis. The results presented in figure 3 are obtained by choosing the stress state corresponding to point 1 of figure 2 as the initial conditions. The ordinate in figure 3 is the derivative with respect to time of the perturbation amplitude, normalized by the initial value of that derivative; the perturbation amplitude is the L_2 norm of the displacement field. This amplitude growth rate is found to be positive. Hence, the perturbation increases with time, but its growth rate always remains of the order of the rate of passive loading if the *in situ* stress σ_0 is less than σ_R. For an *in situ* stress larger than σ_R, the instability develops at a rate that is not controlled by the loading rate.

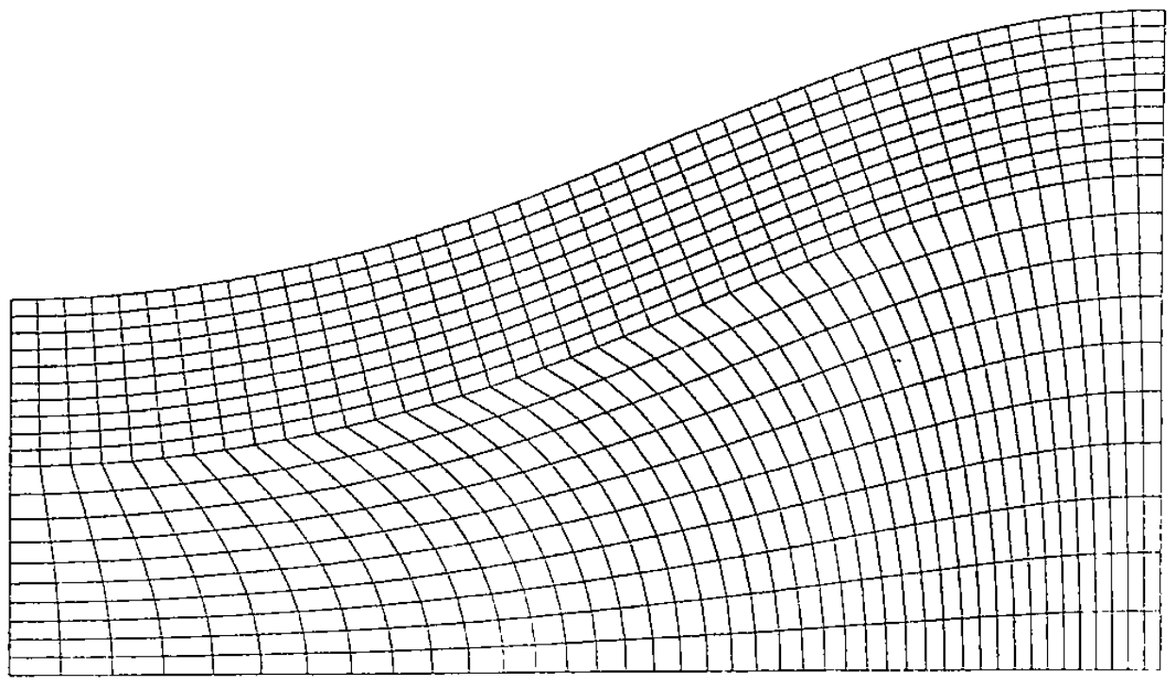

Fig. 4 Final stable equilibrium in the form of a fold resulting from the development of a long-wavelength perturbation in the initially unstable stratified system. The initial substratum to overburden thickness ratio is 2.

Equilibre final stable en forme de pli résultant du développement d'une perturbation de grande longueur d'onde dans un système stratifié initialement instable. Le rapport d'épaisseur entre les couches inférieure et supérieure est de 2.

The development of the instability in the absence of passive loading does not lead to the collapse of the stratified system but to the formation of a stable fold of finite amplitude (**fig. 4**). This new equilibrium depends on the initial *in situ* stress as well as on the type of boundary conditions, as seen in figure 5. For the same initial stress, the fold amplitude A is larger in the case of force control than in the case of displacement

Fig. 5 The fold amplitude A, defined a the vertical distance between crest an trough, as a function of the lateral compressive stress.

L'amplitude du pli, définie comme la distance verticale entre le creux et la crête, en fonction de la contrainte de compression latérale.

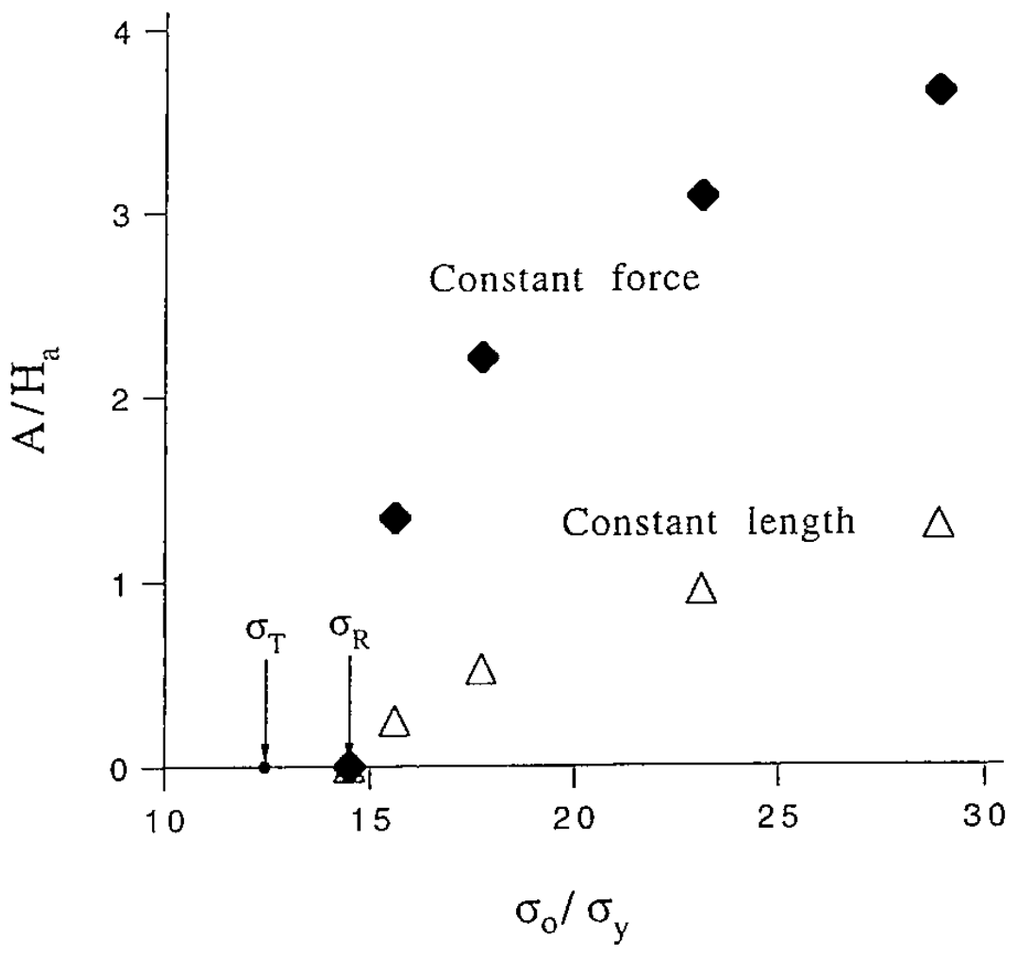

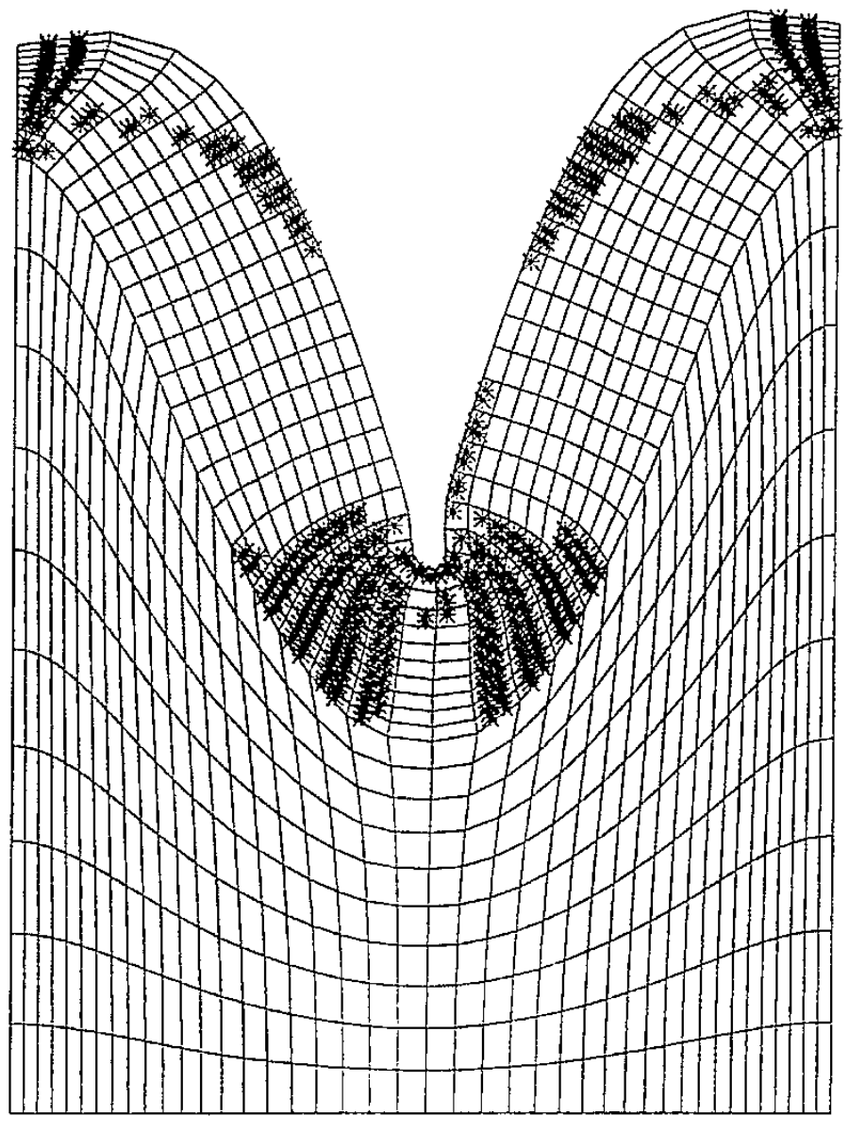

Fig. 6 Collapse of the stratified system in a chevron mode due to faulting. Each star identifies an integration point at which plastic flow is taking place. The initial substratum to overburden thickness ratio is 2.

Ruine du système stratifié en un mode de chevron à la suite de la formation de failles. Chaque étoile indique la position d'un point d'intégration où l'écoulement plastique se produit. Le rapport d'épaisseur entre les couches inférieure et supérieure est de 2.

control. In all cases the new equilibrium is characterized by a fully elastic response of the structure. This restabilization to a new equilibrium does not take place if a loss of ellipticity occurs in the overburden, as happens when σ_0 is larger than σ_R. In that instance, plastic hinges form at the crest and trough of the developing folds and the limbs straighten, resulting in the formation of a chevron. The chevron is not a stable equilibrium if the applied force at the boundary is kept constant. The chevron shown in figure 6 is obtained with two perturbations similar to those of points 2 and 3 in figure 2. The second perturbation had the fastest growth, resulting in the final mode seen in figure 6. In that figure the stars identify the integration points of the finite elements where plastic flow is taking place. Note the localization of the deformation at the hinges. In the presence of a passive compression, the instability development is similar to the one reported above, although the stable fold amplitude continues to increase at a rate governed by the passive loading.

4. CONCLUDING DISCUSSION

The linear stability analysis indicates that the initial compressive stress has to be larger than σ_T in order for the two-layer system to become unstable. The non-linear analysis predicts a critical stress of σ_R which is larger than σ_T (*see* comparison in figure 5). For an *in situ* stress σ_0 larger than σ_R, partial elastic unloading occurs in the overburden as the instability develops at a rate larger than the passive rate of loading. A similar response is found during the loading of the classical rigid T-column model with two discrete elasto-plastic supports (Shanley, 1947; Massin, 1995). This model has received a lot of attention in engineering in view of its simplicity and the potential generalization of its results on stability and bifurcation to the case of continua. A stable bifurcation is detected at σ_T (referred to as the tangent modulus load, in view of the plastic response of the two column supports) and loss of stability occurs at σ_R (denoted the reduced modulus load since one of the supports unloads elastically).

The main difference between the results presented here and those typically obtained with a fluid model is the potential restabilization of a fold. The onset of faulting results in the formation of a chevron for perturbation wavelengths that are long compared to the overburden thickness. Shorter wavelength modes, which could result in collapse mechanisms more reminiscent of a piercement, remain to be explored.

The non-linear analyses should be extended to account for erosion, deposition and compaction of the overburden material. They should also include elasto-plastic models appropriate for monitoring damage development and the initiation of distributed fracture.

Acknowledgments: Part of this work was conducted while one of the authors, Y. M. Leroy, was working for Shell Research, Rijswijk. Permission to publish was granted by Shell Internationale Research Maatschappij.

REFERENCES

BIOT, M.A., 1961. Theory of folding of stratified visco-elastic media and its implication in tectonics and orogenesis, *Geol. Soc. Am. Bull.*, 72, p. 1595-1620.

BIOT, M.A., 1965. *Mechanics of Incremental Deformation*, Wiley, New York, 504 p.

BIOT, M.A. and ODÉ, H., 1965. Theory of gravity instability with variable overburden and compaction, *Geophysics*, 30, pp. 213-227.

HUTCHINSON, J.W., 1973. Numerical solutions of non-linear structural problems, HARTUNG, R.F. *et al.*, ASME, New York, pp. 17-29

HILL, R. and HUTCHINSON, J.W., 1975. Bifurcation phenomena in the plane tension test, *J. Mech. Phys. Solids*, 23, pp. 239-264.

LEHNER, F.K. and KACHANOV, M.L., 1995. On the stress-strain relations for cracked elastic materials in compression, *Mechanics of Jointed and Faulted Rock*, ROSSMANITH, H. P., Ed., Balkena, Rotterdam.

LEROY, Y.M. and TRIANTAFYLLIDIS, N., 1995. Stability of a frictional, cohesive layer on a substratum: variational formulation and asymptotic solution (submitted for publication).

LEMISZKI, P.J., LANDES, J.D. and HATCHER R.D., Jr., 1994. Controls on hinge-parallel extension fracturing in single-layer tangential-longitudinal strain folds, *J. Geophys. Res.*, 99, pp. 22027-22041.

MASSIN, P., 1995. On the stability of rate-dependent solids and structures, *Ph.D. Thesis*, University of Michigan, Ann-Arbor, USA, 203 p.

POIRIER, J.P., 1980. Shear localisation and shear instability in materials in the ductile field, *J. Structural Geology*, 2, pp. 135-142.

PRICE, N.J. and COSGROVE, J.W., 1990. *Analysis of geological structures*, Cambridge University Press.

RICE, J.R., 1976. The localisation of plastic deformation, *Theoretical and Applied Mechanics, Proc. of the 14th IUTAM Conference*, KOITER, W.T., Ed., North Holland, Amsterdam, pp. 207-220.

RUDNICKI, J.W. and RICE, J.R., 1975. Conditions for the localisation of the deformation in pressure-sensitive dilatant materials, *J. Mech. Phys. Solids*, 23, pp. 371-394.

SHANLEY, F.R., 1947. Inelastic column theory, *J. Aero. Sci.*, 14, pp. 261-267.

TRIANTAFYLLIDIS, N. and LEROY, Y.M., 1994. Stability of a frictional material layer resting on a viscous half-space, *J. Mech. Phys. Solids*, 42, pp. 51-110.

TRIANTAFYLLIDIS, N. and LEROY, Y.M., 1995. Stability of a frictional, cohesive layer on a substratum: validation of asymptotic solution and parametric study (submitted for publication).